LAWRENCE
LIVERMORE
NATIONAL
LABORATORY

LLNL-TR-411272

Laser-Driven Dynamic Hohlraums

S. G. Glendinning, J. F. Hansen, R. P. J. Town,
M. C. Herrmann, J. Hammer, R. Heeter

March 16, 2009

Disclaimer

This work performed under the auspices of the U.S. Department of Energy by Lawrence Livermore National Laboratory under Contract DE-AC52-07NA27344.

FY08 LDRD Final Report
Laser-Driven Dynamic Hohlraums
LDRD Project Tracking Code: 06-ERD-017
S. G. Glendinning, Principal Investigator

Abstract

A novel approach for laser-driven inertial confinement fusion is described, that of the laser-driven dynamic hohlraum. Combining direct and x-ray drive, the laser-driven dynamic hohlraum uses a radiatively collapsed shock to confine x-radiation and drive an inner capsule. Ignition is predicted for such a system on the National Ignition Facility. In this LDRD the laser-driven dynamic hohlraum was experimentally investigated on the Omega laser. . In addition, the laser-driven dynamic hohlraum was investigated as a possible bright, short duration, continuum x-ray source suitable for opacity experiments. Results from these dynamic hohlraum experiments are presented, showing both agreement with and discrepancies with simulations.

Introduction/Background

Radiatively collapsed shocks[i] are a well-known feature of the interstellar medium [iiiiiivv]. A shock is termed "radiative" when the energy lost to radiation becomes significant; as the radiation heats the surrounding medium, the shock material cools and becomes denser. In the regime where the radiation heats material both upstream and downstream of the shock, the result is a nearly isothermal system. The solution of the Rankine-Hugoniot equations is simple in an isothermal system, and predicts that the compression of the shocked region is equal to the Mach number squared. Radiative shocks have recently been produced in several high energy density experiments in the laboratory[viviiviii], and radiatively collapsed shocks have been observed in a laser-driven system in planar geometry [ixx].

One important laboratory application of a radiative shock is the Z-pinch driven dynamic hohlraum (DH) [xixii]. In this application, the energy of the Z-pinch (in this case the Z-machine at Sandia), is dumped into a cylindrical array of tungsten wires, which then implode. The x-radiation from the wires is confined by the opaque wires, resulting in a blackbody radiation cavity or hohlraum. In the dynamic version, the wire array collides with a coaxial cylinder of CH foam, launching a radiative shock. The radiation from the shock results in an additional x-ray source (by converting the kinetic energy of the wires to radiation), which results in a higher blackbody temperature of the drive. These dynamic hohlraums have resulted in the increase of temperatures from ~155 eV [xiii] to ~215 eV [11], about a threefold increase in x-ray flux over the conventional hohlraum.

It is at first difficult to imagine how one might apply the dynamic hohlraum concept to laser driven inertial confinement fusion (ICF). Laser driven ICF [xiv] is usually considered to comprise two approaches: direct drive, in which laser light directly ablates the surface

of a capsule; and indirect drive, in which laser light is converted to x-rays through the use of a high-Z hohlraum and the x-rays ablate the surface of a capsule. In both cases, the capsule must be uniformly irradiated to converge to the high density required to ignite the thermonuclear fuel (a mixture of deuterium and tritium) contained in the capsule. The hohraum wall however is illuminated internally and is essentially stationary throughout the laser pulse (eventually of course it accelerates outward), so there is no obvious analogue to the imploding wire array. The solution is the configuration shown in Figure 1. A thin-walled, low-Z, spherical capsule is uniformly illuminated with a laser (just as in the direct-drive version of laser-driven ICF). The ablation launches a shock which quickly traverses the ablator and enters a high-Z, low density gas fill. Reighard et al. in Ref. 11 have derived that a shock in this density of Xe becomes radiative when the velocity of the shock exceeds 50 km/s. The shock in the high-Z gas is a radiative shock which radiatively collapses and becomes opaque to the shock radiation. The convergent shock forms a dynamic hohlraum as the volume shrinks as a function of time. In the configuration shown in Figure 1, the laser-driven DH is used to drive a capsule; x-rays from the radiatively collapsed shock ablate surface material from the capsule, which implodes just as a radiatively driven capsule in a traditional, internally illuminated hohlraum. In addition, the material ablated from the capsule surface and the converging RC shock stagnate against each other, converting their kinetic energy to radiation, increasing the drive just as in the Z-pinch driven DH. The drive is sufficient that an implosion of this type is predicted to achieve ignition using the NIF, without the use of cryogenic fuel as required in the NIF point ignition design [[xv]]. While similar in appearance to the indirectly driven double-shell implosions proposed by Amendt et al.,[xvi] this capsule is predicted to be less sensitive to the Rayleigh-Taylor instability due to the radiative drive of the inner shell.

Another application for the laser-driven DH which was explored was its possible use as a spectrally smooth backlighter. Opacity and temperature measurements in hot, dense plasmas are of vital importance in understanding and predicting plasma evolution in high energy density physics experiments. Perry[xvii] demonstrated that plasma temperatures may be determined by including a dopant material and measuring its x-ray absorption spectrum near the K-edge. As the temperature of the plasma increases, the K-edge of the material used must be at a higher energy. The challenge lies not in choosing the dopant material, but in finding a suitable x-ray source to backlight the plasma for the absorption measurement. Previous researchers[xviii],[xix] have used hydrogen-filled plastic capsules, driven symmetrically of the Omega laser, as backlighter sources. In these sources, the predominant emission comes from bremsstrahlung in the imploded plastic shell. It is plausible that augmenting the shell emission with higher-Z materials would produce brighter sources at higher x-ray energies. However, adding solid materials to the shell usually results in line emission from embedded layers, making the emission less suitable for a spectrally resolved absorption measurement.

Research Activities – Ignition targets

I – Radiative shock

The first experiment was the demonstration of the conditions required for a laser-driven DH; that is, the presence of a strongly radiative, collapsed shock. In this experiment 40 beams of the Omega laser were used to implode a CH capsule with an initial outer radius of 485 μm and a wall thickness of 20 μm, filled with 1.5 atm Xe. The laser pulse duration was approximately 1.1 ns (FWHM) at about 14 TW of 0.35 μm light, and all 40 beams were smoothed with distributed phase plates and spectral dispersion [xxxxxi]. Ten of the remaining 20 beams of the laser were used to generate an x-ray radiography source by illuminating a Ti foil, producing predominately He-α x-rays at 4.7 keV. The resulting radiography was imaged with a 20 μm slit and projected on an x-ray streak camera, generating the streaked radiograph shown in Figure 2. The velocity of the shock is greater than 50 km/s (the threshold for radiative effects as mentioned above) by about XX ns and peaks at about 300 km/s in these experiments. As the shock in the Xe radiates and collapses, it heats the remaining CH of the capsule wall, resulting in the transmissive region noted in Figure 2.

In Figure 3 we show comparisons between simulations of the result shown in Figure 2, with and without radiation present in the problem. All the simulations described here were done with the two-dimensional radiative hydrodynamics code LASNEX [xxii], and the results were post-processed with the backlighter spectrum and instrument response to produce simulated radiographs. The simulated radiographs were analyzed in the same manner as the measured radiographs. In Figure 3a we show the width of the heated trasmissive region as a function of time, and in Figure 3b the width of the shock in the Xe is plotted. The heated transmissive region is present to some degree even without a radiative shock, due to heating by electron conduction; however, the heated region is considerably larger in the presence of radiation from the shock. The width of the shock in Xe is also larger if no radiation is present in the problem. In these simulations, the Mach number of the shock in the Xe is about 7-10, so the anticipated compression of the shocked Xe is about 50-100 when it is radiatively collapsed. (In the simulations with radiation, the compression is about 100-150, suggesting that the isothermal estimate of compression is an oversimplification.) The time evolution of the width of the transmissive region from the simulations with and without radiation is compared with that of the experimental radiograph in Figure 3a. The simulation including radiation agrees with the data within the error bars, showing the presence of the radiative shock. The width of the compressed Xe region from the simulations and the experiment is shown in Figure 3b, again agreeing with the simulation with radiation and showing the reduced width anticipated from the radiatively collapsed shock.

II – Symmetric implosions

Experiments were then conducted using the laser-driven DH to implode an inner capsule. The parameters of this target are listed in Table I. In this case all 60 beams of the Omega laser were used to drive the capsule, using about 22.8 TW of 0.35 μm light. The simulations of this system predict two bursts of neutron production, with the first due to the radiative drive of the capsule, and the second due to the collision of the outer shell with the inner shell. The yield from each of the two bursts (without including the effects of mixing cold shell material into the fuel) would be approximately equal. It is possible to estimate the effects of mix on the two bursts of neutrons by using a fall line analysis

[xxiiixxivxxv]. In this analysis, the sensitivity of an implosion to mix is determined by the time between the earliest arrival of shell material at the center and the peak neutron production time, normalized to the time between the peak velocity time and the peak neutron production time, as

$$\Delta\tau = \left(\frac{r(t_0)}{v_{imp}} + t_0 - t_b \right) \Big/ \delta t \qquad (1)$$

where t_0 is the time of peak shell velocity, $r(t_0)$ is the shell radius at this time, v_{imp} is the peak shell velocity, t_b is the time of peak neutron production, and $\delta\tau = t_0 - t_b$. Thus, $\Delta\tau < 0$ corresponds to an implosion which should be less sensitive to mix as most neutrons are produced before the shell material can reach the center, while $\Delta\tau > 0$ corresponds to an implosion which would be more sensitive to mix. In the simulations of the laser-driven DH implosions, the two bursts of neutrons have $\Delta\tau$ of -0.4 for the ablatively driven burst and +1.7 for the second burst of neutrons. An empirical evaluation of the yield reduction as a function of fall line behavior from Ref. 21 predicts a yield reduction to 45-80% of clean yield for the ablative neutrons, but a reduction to 2-5% of clean yield for the second burst of neutrons.

In addition to the yield, the fuel and shell areal densities at the time of neutron production are also affected by mix. The measured areal density[xxvi] is the weighted average of the time-dependent areal density weighted by the neutron production history; thus if the second burst of neutrons is suppressed, the areal density will be approximately the areal density at the time of the first burst of neutrons. Table II shows the comparison of the simulated fuel and shell areal density with and without mix from the simulations and the measured fuel and shell areal density. The same prediction is also shown for the system with radiation turned off, also with and without including the effect of mix; the experiments agree with the simulation including radiation within error bars, whereas the simulations without radiation are well outside the error bars.

These results were encouraging and prompted the next experimental effort, minimizing the effect of radiation by replacing the gas in the DH with neopentane (C_5H_{12}). While this is not an exact analogue to the no-radiation case which can be addressed in the simulation, the important point is that the shock in the neopentane does not radiatively collapse. The implosion parameters for this "colliding shell" implosion are also shown in Table II. The simulated fuel and shell areal densities were significantly higher than those for the radiatively driven implosions; the difference between the neopentane and Xe filled shells should have been well within the experimental uncertainty of the diagostic. Surprisingly, the fuel areal densities was lower by a factor of about five than the simulated values. To date, no adequate explanation for this discrepancy has been found. It should be noted that the discrepancy does not exist with the dynamic hohlraum targets, but with the targets which minimized the radiative drive. However, the discrepancies

throw some doubt on the mix explanation of the dynamic hohlraum results. Much more work would need to be done to improve the understanding of these implosions.

III – Polar Direct Drive

The laser-drive DH is intended as an alternative ignition target for NIF. However, NIF is configured for the beams to uniformly illuminate the interior of a cylindrical hohlraum, not the surface of a sphere. A considerable amount of work has been done at the Laboratory for Laser Energetics to optimize the NIF beam configuration for direct drive, by repointing the beams and tuning the pulse shapes[xxvii],[xxviii]. The laser-driven DH can take advantage of these studies (known as the Polar Direct Drive technique) to design a symmetric implosion using asymmetric laser beam configuration. A series of experiments was performed on the Omega laser using targets nominally identical to the Xe-filled targets described above. The laser was configured to use only 40 of the 60 beams, removing those providing symmetric illumination at the chamber equator. This is a configuration very similar to that available on the NIF. The beams were then repointed to positions designed to provide a more symmetric implosion. The implosion symmetry was diagnosed by x-ray pinhole framing cameras, giving a series of 2D images with a temporal resolution of 40 ps and spatial resolution of about 15 μm. A typical sequence from a pointing designed to give a symmetric implosion is shown in Figure 4. The outer plastic shell of the target emits in x-rays as it is ablated by the laser drive. In the early time images, the inner capsule may be seen silhouetted by this x-ray emission. The outer shell is fairly round as it implodes, although a thin plate of beryllium used to plug the outer shell after the inner shell is inserted (visible in the lower left of each frame) introduces an asymmetry in that direction. Later in time the inner shell is observed to emit in x-rays as it is heated and ablated by both the x-ray drive and the collision with the outer shell. The distortion of the outer shell is measured from each image (defined to be the coefficient of the second Legendre mode divided by the radius at that time) and the result is show in Figure 5 for this shot. The distortion is small, less than a few percent at all times. The simulated distortion is also shown, and agrees with the data.

Table I. Capsule characteristics for Omega experiments and NIF ignition designs.

Capsule	Low-Z ablator			Outer capsule fill	High-Z ablator			Inner capsule fill
	Outer radius	Inner radius	Mat'l		Outer radius	Inner radius	Mat'l	
Omega	0.0485 cm	0.0476 cm	CH 1.05 g/cm^3	Xe 0.009 g/cm^3	0.0250 cm	0.0225 cm	SiO_2 4. g/cm^3	D_2 0.018 g/cm^3
Omega	0.0485 cm	0.0476 cm	CH 1.05 g/cm^3	C_5H_{12} 0.004 g/cm^3	0.0250 cm	0.0225 cm	SiO_2 4. g/cm^3	D_2 0.018 g/cm^3
NIF	0.2925 cm	0.2900 cm	CH 1.05 g/cm^3	Xe 0.009 g/cm^3	0.0430 cm	0.0380 cm	Au/Cu 19 g/cm^3	DT 0.13 g/cm^3

Table IIa. Implosion results using laser-driven dynamic hohlraums (Xe filled).

	Simulation (no radiation)		Simulation (with radiation)		Experiment
	No mix	With mix	No mix	With mix	
Fuel ρr (mg/cm^2)	31.6	29.0	17.4	**5.3**	**4.5±0.5**
Shell ρr (mg/cm^2)	171	159	92.	**35.5**	**40±7**
Yield (10^9 neutrons)	196	56	37.4	**12.7**	**3.0±0.5**

b) Implosion results using laser-driven shell collisions (C_5H_{12} filled).

	Simulation (with radiation)		Experiment
	No mix	With mix	
Fuel ρr (mg/cm^2)	16.0	**12.7**	**2.3±0.3**
Shell ρr (mg/cm^2)	89.5	**75.6**	**60±8**
Yield (10^9 neutrons)	40.0	**15.5**	**3.2±0.5**

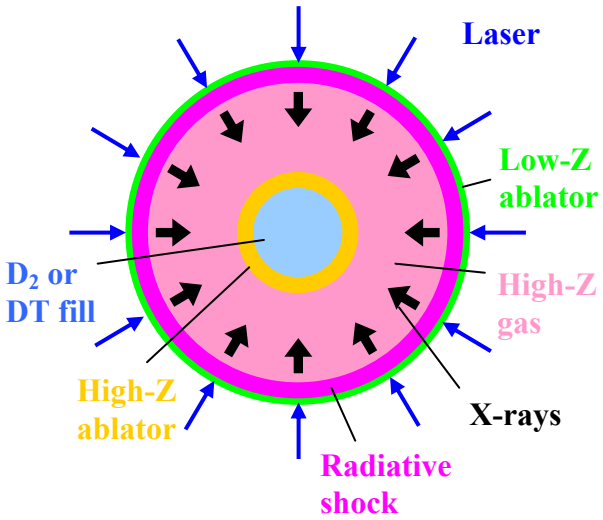

Figure 1. Schematic of the laser-driven dynamic hohlraum with an inner capsule. The blue arrows represent a uniform laser illumination of the low-Z ablator (green). This drives a radiative shock (violet) into the high-Z gas (light violet). The radiative shock produces x-rays (black arrows), which, in turn, ablate a high-Z inner capsule (gold), filled with D_2 or DT (blue) at high pressure.

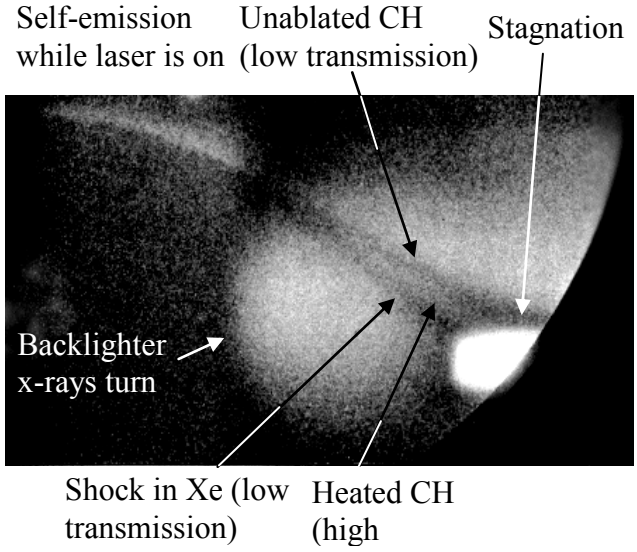

Figure 2. X-ray streak camera image of an imploding dynamic hohlraum.

a)

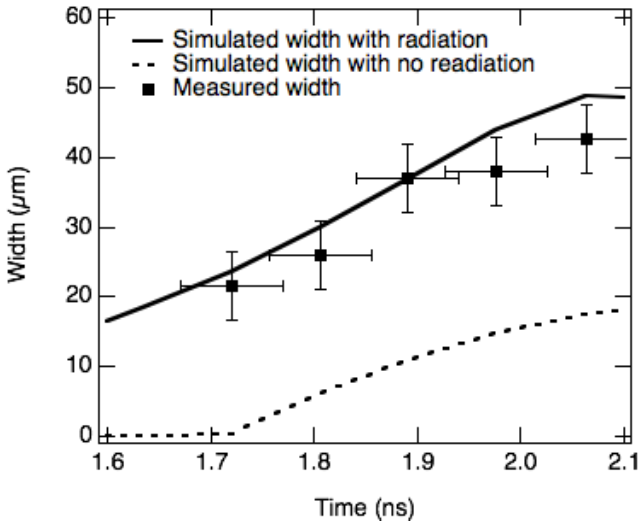

b)

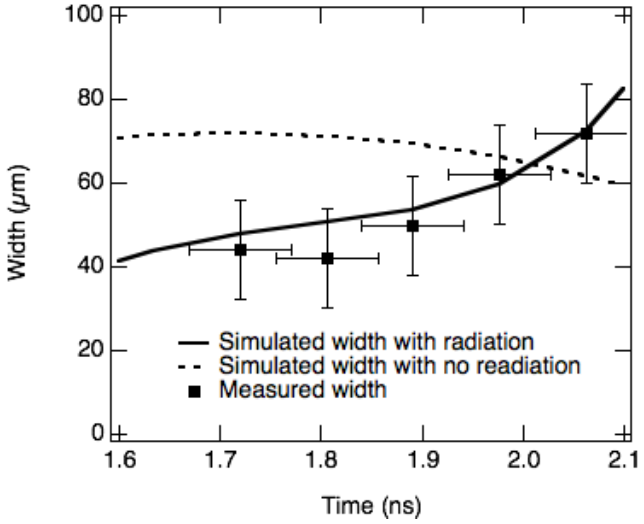

Figure 3. a) Measurement (squares with error bars) of the width of the transmissive region shown in Figure 2 as a function of time. Simulations with (solid) and without (dashed) radiation are also shown. b) Same conditions as a, for the width of the shocked region in the Xe.

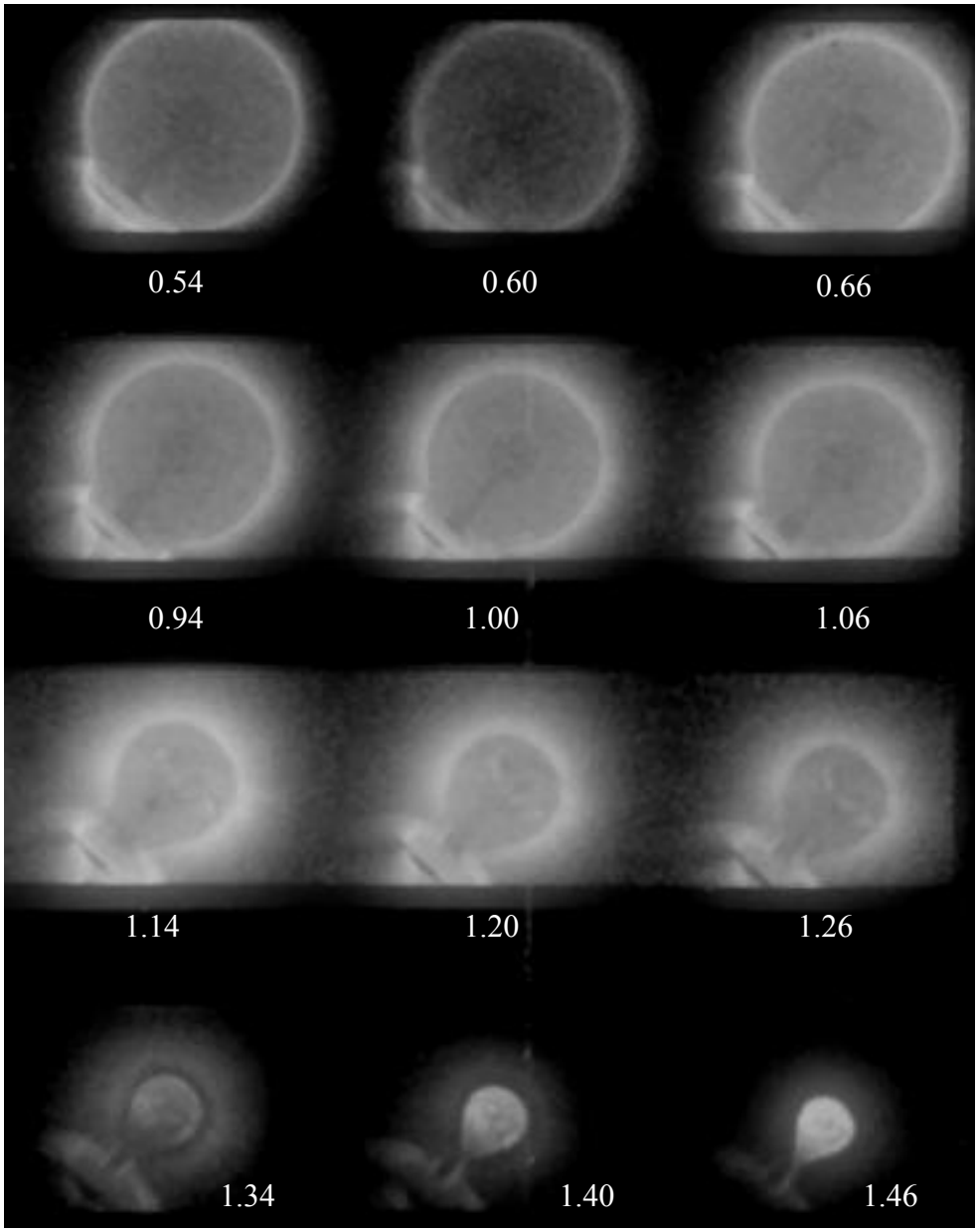

Figure 4. A temporal sequence of images from a polar direct-drive experiment. The time of the frame from the beginning of the laser pulse (in ns) is shown below each frame.

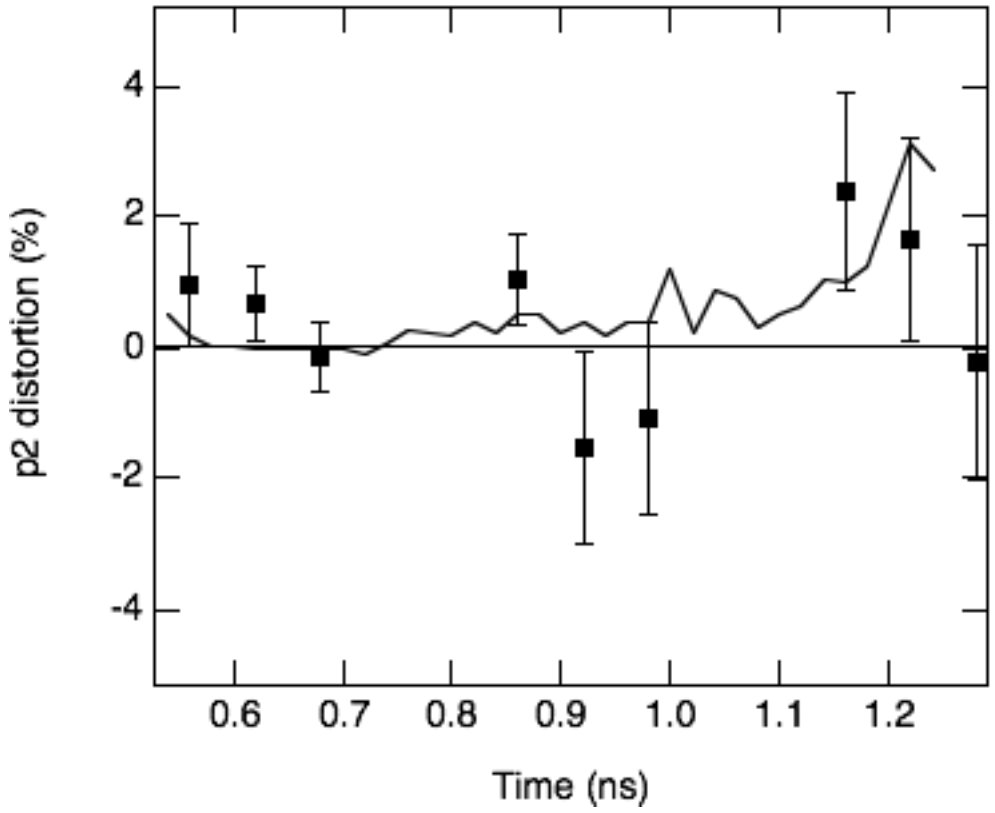

Figure 5. Distortion as Legendre mode P2/radius in percent vs time. The squares are the data and the solid line is from simulated images.

Research Activities – Backlighter targets

Laser-driven DH targets were designed specifically for backlighter experiments; they were smaller than the ignition-relevant targets (as most of the laser beams are used to heat the plasma to be diagnosed), and there was no inner capsule. The targets comprised 380 μm diameter capsules with 9.2 μm thick walls, filled with krypton or argon for the DH, and filled with hydrogen as a null comparison. The capsules were driven with ten of the Omega laser beams, using a 600 ps square pulse. The illumination of the capsule is not predicted to be uniform with only ten beams with the intensity at the poles about two-thirds that at the equator.

Three parameters are of considerable importance in determining the suitability of an x-ray backlighter for opacity experiments: emission source size, emission duration, and spectral shape. The requirements are that the source size be <~ 100 μm, and that the optimum emission duration be 80-230 ps. The spectral smoothness requirement is set indirectly by the noise requirements on the signal, that at least ~300 photons are detected per spectral resolution element. Thus, any spectral minima must exceed this signal level, without spectral maxima exceeding the diagnostic dynamic range. The requirement for the instruments used is ±6%.

The experiments were diagnosed with three primary diagnostics to determine emission spatial extent, temporal duration, and spectral content. These were an x-ray framing camera (identical to that used in the implosion experiments), a streaked x-ray spectrometer, and a gated (spatially resolving) x-ray spectrometer. The streaked spectrometer covered a photon energy ranging from 3.4 to 5.4 keV with a 4 ns long time window (calibrated on separate shots and with a dopant added to one capsule). The gated spectrometers (three were used) are the same instruments used for opacity experiments[xxix],[xxx]. These consist of elliptical and flat crystals that reflect (through Bragg diffraciton) x-rays from a source to an imaging element consisting of a gated microchannel plate. The use of elliptic rather than flat crystals provides a means of focusing x-rays from spatially extended sources. In addition, the absolute emission was measured using the Dante broadband x-ray spectrometer[xxxi]

The results of the experiments are shown in Figure 6 (temporal duration), Figures 7 a and b (simulated and measured spatial extent), Figure 8 (spectral response), and Figure 9 (absolute emission). All capsules (Kr, Ar, and H_2 filled) gave similar temporal duration (about 60-100 ps). All capsules also gave similar spatial size (about 50-70 μm). The effect of the nonuniform laser illumination may be seen in Figures 7 a and b; note that at the time of peak brightness the distortion is small (~25%), allowing the capsules to meet the spatial extent specification of <100 μm.

A second set of experiments was fielded to examine the maximum spectral extent of the DH backlighter, used with 40 of the Omega beams in the polar direct drive configuration described above. One elliptical spectrometer was reconfigured to cover a spectral range from 4.5 to 9.0 keV. In addition two other elliptical spectrometers covered spectral ranges from 1.2 2 keV and 3 – 5.5 keV. All spectrometers showed smooth spectra with signals which met the requirements for opacity experiments.

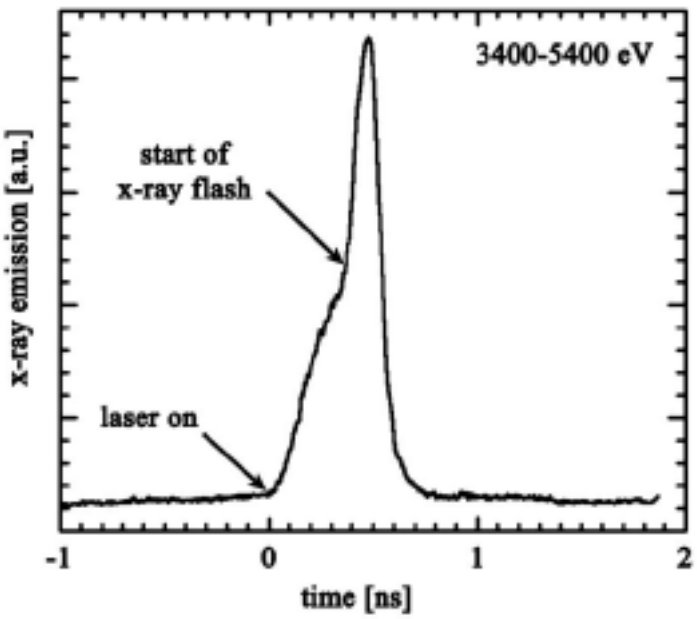

Figure 6. Line out of the streaked spectrum on the Kr-filled dynamic hohlraum target showing the bright x-ray flash. The lineout is over a broad spectral range, artificially broadening the temporal duration.

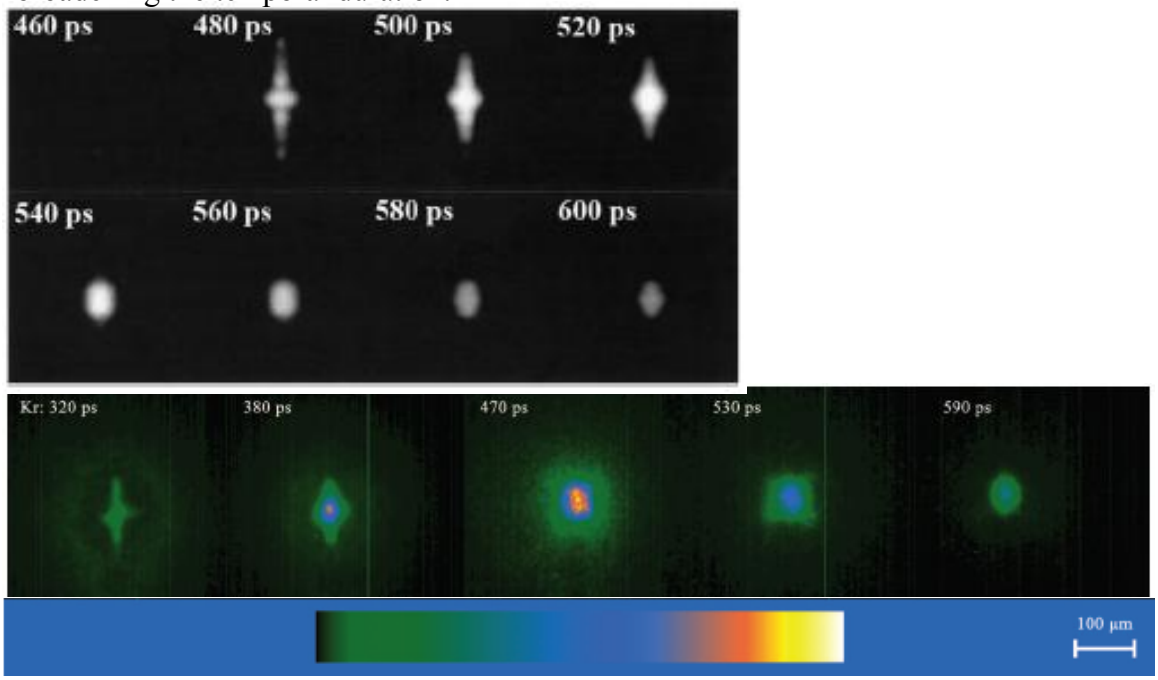

Figure 7. a) Simulated and b) measured spatially and temporally resolved emission from the Kr capsule. The laser drive is weaker at the poles, resulting in two opposing jetlike structures.

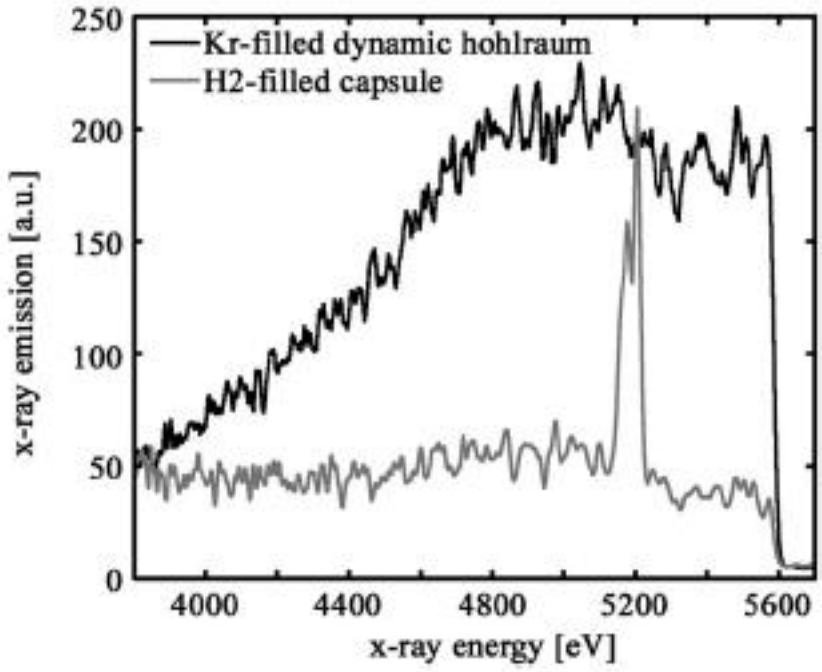

Figure 8. Gated spectrometer data from a Kr-filled dynamic hohlraum and an H_2-filled capsule. The spectra from the dynamic hohlraums were sufficiently smooth (rms noise < 6%) to satisfy requirements for opacity experiments; the less bright H_2-filled capsules were not. The line feature for the H_2-filled capsule is a vanadium He-a line from a small quantity of dopant added to the shell.

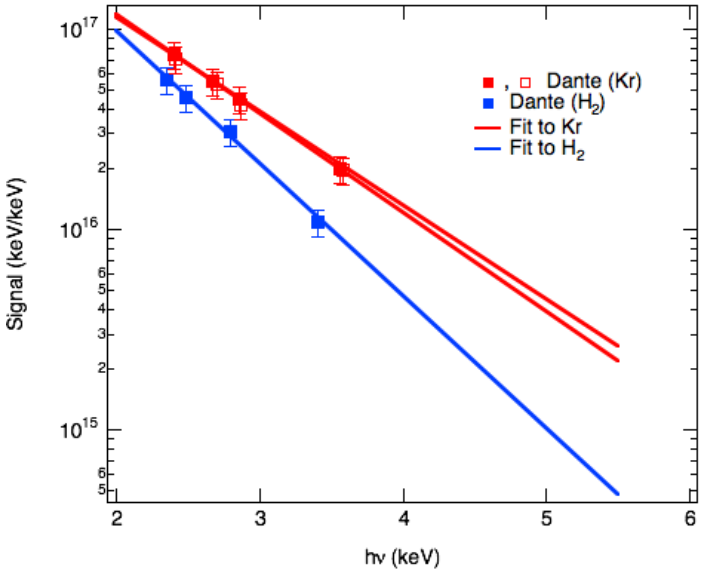

Figure 9. Emission spectra from the Dante broadband spectrometer. The straight lines are bremsstrahlung (exponentially decaying) fits to the signals)

Exit Plan

We have several academic collaborators from the laboratory astrophysics community who are interested in using the dynamic hohlraum backlighter to characterize a hot plasma by measuring the absorption spectrum of a plastic-tamped, laser-heated non-LTE iron sample. Preliminary experiments and simulations carried out in the last year of the LDRD are very promising, showing that the backlighter has the necessary spectral extent to cover the required regime. While tests in the preliminary experiments did not raise the iron sample to the required conditions, this is simply a matter of iterating on the conditions which were achieved with refined simulations. Our collaborators are interested in applying for NLUF experiments.

The dynamic hohlraum backlighters are planned to be used in several experiments beyond the opacity experiments for which they were originally intended. Spectrally smooth sources are also required for EXAFS measurements and Laue diffraction measurements. Both of these techniques will be utilized in dynamic materials science studies to be performed on the NIF, and the DH backlighters are the current best candidates for this programmatic work.

The possibility of the laser-driven DH as a novel ignition target would require considerable further study before implementation on the NIF would be practical. Currently there is no realistic funding source for continuing these studies.

Summary

The laser-driven dynamic hohlraum has been shown to represent a novel system for imploding capsules, qualitatively different from colliding double-shell capsules. The radiatively collapsed shock in the Xe fill of the outer capsule has been observed to heat the capsule walls as predicted; the capsules perform as predicted (for an assumed mix model which relies on simulations of the shell trajectories and burn history), and the fuel and shell areal densities agreed with predictions. In additions, good symmetry was achievable using an asymmetric laser drive.

However, the inability of the simulations to predict similar capsules with reduced radiative drive throws doubt on the validity of the mix model used. Whether the flaw lies with the assumptions of the model or the simulations of the shell trajectories and burn history is not clear. It is not clear at the conclusion of this work whether an ignition design for the NIF is plausible.

The laser-driven dynamic hohlraum has earned a place as a near-ideal backlighter for opacity experiments. It may be used with a small part of the laser energy, allowing most of the energy to be used to drive the main experiment; it is relatively insensitive to laser asymmetry for this purpose, and it has sufficient signal and spectral smoothness to facilitate opacity measurements at required precisions. It is currently fielded routinely in opacity experiments at Omega and will continue on the NIF.

References

[i] R. P. Drake, Astrophysics and Space Science **298**, 49 (2005).
[ii] K.J. Borkowski, J.M. Blondin and R. McCray, ApJ. **477**, 281 (1997).
[iii] N. Calvet and E. Gullbring, ApJ. **509**, 802 (1998).
[iv] L. Ensman and A. Burrows, ApJ., **393**, 742 (1992).
[v] R.A. Chevalier, Science **276**, 1374 (1997).
[vi] P. A. Keiter et al.; Phys. Rev. Lett. **89**, 165003/1 (2002).
[vii] J. Grun et al., Phys. Rev. Lett. **66**, 2738 (1991).
[viii] M. J. Edwards et al., Phys. Rev. Lett. **87**, 085004/1 (2001).
[ix] S. Bouquet et al., Phys. Rev. Lett. **92**, 22500/1 (2004).
[x] A. B. Reighard et al, Phys. Plasmas **13**, 082901/1 (2006).
[xi] M. K. Matzen et. al, Phys. Plasmas **12**, 055503/1 (2005).
[xii] D. D. Ryutov et al., Rev. Mod. Phys. **72**, 167 (2002).
[xiii] M. K. Matzen et al., Plasma Phys. Controlled Fusion **41**, A175 (1999).
[xiv] J. Lindl Indirect drive fusion
[xv] S.W. Haan et al., Phys. Plasmas **2** 2480 (1995).
[xvi] P.A.Amendt et al., Phys. Plasmas **9** 2221 (2002).
[xvii] T.S. Perry et al., Phys. Rev. Lett. **67** 3784 (1991).
[xviii] B. Yaakobi et al., J. Opt. Soc. Am. B **20**238 (2003).
[xix] B. Yaakobi et al., Pyhs. Rev. Lett. **92**, 095504 (2004).
[xx] Y. Lin et al., Opt. Lett. **20**, 764 1995.
[xxi] S. Skupsky et al., J. Appl. Phys. 66, 3456 1989.
[xxii] G. Zimmerman and W. Kruer, Comments Plasma Phys. Control. Fusion **2**, 85 (1975).
[xxiii] P. Amendt et al., Phys. Plasmas **9** 2221 (2002).
[xxiv] H. F. Robey et al., Phys. Plasmas **12** 072701 (2005).
[xxv] J. L. Milovich et al., Phys. Plasmas **11** 1552, (2004).
[xxvi] C.K.Li et al., Phys. Plasmas **7** 2578 (2000).
[xxvii] S. Skupsky *et al.*, Phys. Plasmas **11** 2763 (2004).
[xxviii] R. S. Craxton *et al.*, Phys. Plasmas **12** 056304 (2005).
[xxix] R.F.Heeter et al., Re. Sci. Instrum **75**, 3762 (2004).
[xxx] M. May, R. Heeter, and J. Emig, Rev. Sci. Instrum. **75**, 3740 (2004).
[xxxi] H.N.Kornblum, R.L.Kauffmann, and J.A.Smith, Rev. Sci. Inst. **57** 2179 (1986).